Status and performance of the Discovery Channel Telescope during commissioning

Stephen E. Levine[a,*], Thomas A. Bida[a], Tomas Chylek[a], Peter L. Collins[a], William T. DeGroff[a], Edward W. Dunham[a], Paul J. Lotz[a], Alexander J. Venetiou[a], and Saeid Zoonemat Kermani[a]

[a]Lowell Observatory, 1400 West Mars Hill Road, Flagstaff, AZ 86001, USA

ABSTRACT

Lowell Observatory's Discovery Channel Telescope is a 4.3m telescope designed for optical and near infrared astronomical observation. At first light, the telescope will have a cube capable of carrying five instruments and the wave front sensing and guider system at the f/6.1 RC focus. The corrected RC focus field of view is 30′ in diameter. Nasmyth and prime focus can be instrumented subsequently. Early commissioning work with the installed primary mirror and its support system started out using one of the wave front sensing probes mounted at prime focus, and has continued at RC with the recent installation of the secondary mirror. We will report on the on-sky pointing and tracking performance of the telescope, initial assessment of the functionality of the active optics support system, and tests of the early image quality of the telescope and optics. We will also describe the suite of first light instruments, and early science operations.

Keywords: DCT, Discovery Channel Telescope, Lowell Observatory, Commissioning, System Status

1. INTRODUCTION

Lowell Observatory's 4.3-meter Discovery Channel Telescope is in the process of being commissioned now. The telescope is located 40 miles southeast of Flagstaff, at Happy Jack, AZ (Longitude: 111:25:21.054 W, Latitude: 34:44:39.498 N, Elevation: 2337 meters referenced to WGS84, retrieved from the site GPS receiver, 2012 June 15). On sky testing of the major subsystems began in September 2011, with commissioning work leading up to first light in late spring of 2012. Early science operations for Lowell and its partner institutions, Boston University, the University of Maryland, and the University of Toledo, are on track to begin in early 2013.

The telescope has the capability to carry instruments at the Nasmyth, Prime and RC Cassegrain foci. At first light, the telescope will have a cube capable of carrying five instruments and the wave front sensing and guider system at the f/6.1 RC focus. The corrected RC focus field of view is 30′ in diameter. The mount was built by General Dynamics, and the telescope control system (designed around the TCSpk and TPOINT pointing kernel from Tpoint Software[1]) was done by Observatory Sciences Ltd. (OSL). The wavefront sensing system and active optics systems were designed and implemented at Lowell.

The primary mirror (M1) is a thin meniscus mirror. It is 4.3-meters in diameter, 4-inches thick, cast from ULE, and has an f/1.9 focal ratio. The secondary mirror (M2) is a lightweight honeycomb design, 1.4-meters in diameter. Both optics are finished, aluminized and installed in the telescope. The active optics system (AOS) controls the alignment of both optics, and also maintains the correct figure of the primary. These will be corrected twice a minute using data from the integrated Shack-Hartmann wave front sensing system.

Site testing work at the DCT site at Happy Jack, AZ showed that the median site seeing over 117 nights was 0.″84, and the first quartile average was 0.″62.[2] Image quality has been between 0.″9 and 1.″1 FWHM without any wavefront correction. Correcting for Zernikes 4 through 11 (focus, coma, astigmatism, trefoil and spherical) has improved the FWHM to between 0.″8 and 1.″0. When coupled with the telescope's pointing and tracking model, we are able to take 5 minute long unguided images with sub-arcsecond FWHM.

*Corresponding author: E-mail: sel@lowell.edu, Telephone: +1 928 774 3358

Levine, S. E., et al., "Status and performance of the Discovery Channel Telescope during commissioning", in Ground-based and Airborne Telescopes IV., Proc. of SPIE, 8444-44 (2012),

2. TELESCOPE SYSTEMS OVERVIEW

The Discovery Channel Telescope facilities comprise a complete astronomical observatory, including a telescope building, auxiliary building, astronomers lodge, and support equipment.

2.1 Mechanical

The telescope building includes a fixed base structure and a rotating dome (Fig. 1, left). The base structure contains a control room, computer room, instrument maintenance space, electrical equipment room, and receiving bay on the first floor. The second floor has all the necessary utilities to support instruments; at the moment it is used for largely for storage and additional workspace. The facility includes a hydraulic personnel lift and double bridge crane on the observing level to facilitate maintenance activities for the telescope and dome. The rotating dome[3] is an octagonal steel structure with flat facets and a bi-parting shutter system. The dome is covered with aluminized foil for improved thermal performance. Both the second floor and the observing level include roll-up doors to help with thermal equilibration.

Figure 1. *Left:* The DCT enclosure. The dome shutter is open, as are the observing level vent doors. The second floor vent doors are the panels just below the bottom of the dome. *Right:* The DCT Mount.

An auxiliary building provides space for maintenance and coating of the optics, and all of the major support equipment, including the facility and instrument chillers, and a diesel-powered backup generator, which permits us to gracefully shutdown the facility in the event of a prolonged power outage. The mirror coating chamber was used to coat the both primary and secondary mirrors. It is an up looking chamber, built by DynaVac.[4] All mount motors are cooled by the glycol system to eliminate thermal plumes which could contribute to degraded seeing. Heat collected by the glycol is vented to the atmosphere at the instrument chiller.

The mount[5] (Fig. 1 right) is a conventional altitude over azimuth configuration, designed and fabricated by General Dynamics SATCOM Technologies (GDST) in Richardson, Texas. The mount is controlled by GDSTs proven Model 133 control system. This system is very similar to that provided for both the VISTA and SOAR telescopes, with minor changes made to accommodate the DCT hardware design and performance. The azimuth drive train is built up from two pairs of two motors and gear reduction boxes; the elevation axis is driven by two direct drive motors, one each on the top of the fork arms. The Cassegrain rotator is driven by a pair of counter-torqued motors, similar to the Azimuth motors. The Cassegrain cable wrap is slaved to the rotator and driven by a single motor. We have already verified that we can run the mount in a functional mode on a less than a complete complement of motors.

2.2 Optical

The telescope optics[6] include the 4.3-meter primary mirror, figured by the University of Arizona Optical Sciences Center, and a 1.4-meter secondary mirror figured by L-3 Integrated Optical Systems – Brashear. Based on a stray light analysis of the optical system, a system of baffles and stops was designed and fabricated to minimize stray light.

The Active Optics System (AOS)[7] comprises the actuators, sensors, and controls necessary to maintain the figure and alignment of the telescope mirrors. The primary mirror is controlled by 120 axial electromechanically-driven ballscrew actuators (each consisting of a stepper motor, harmonic drive and screw actuator), 36 lateral pneumatic actuators in a Schwesinger style configuration,[8] and three tangential definers (the layout is shown schematically in Fig. 2). Three tangent definers provide the force feedback required to control the lateral supports and define the M1 position in x, y and rotation. The primary mirror is actively cooled by a cold plate using a chilled water-glycol mixture from the instrument chiller.

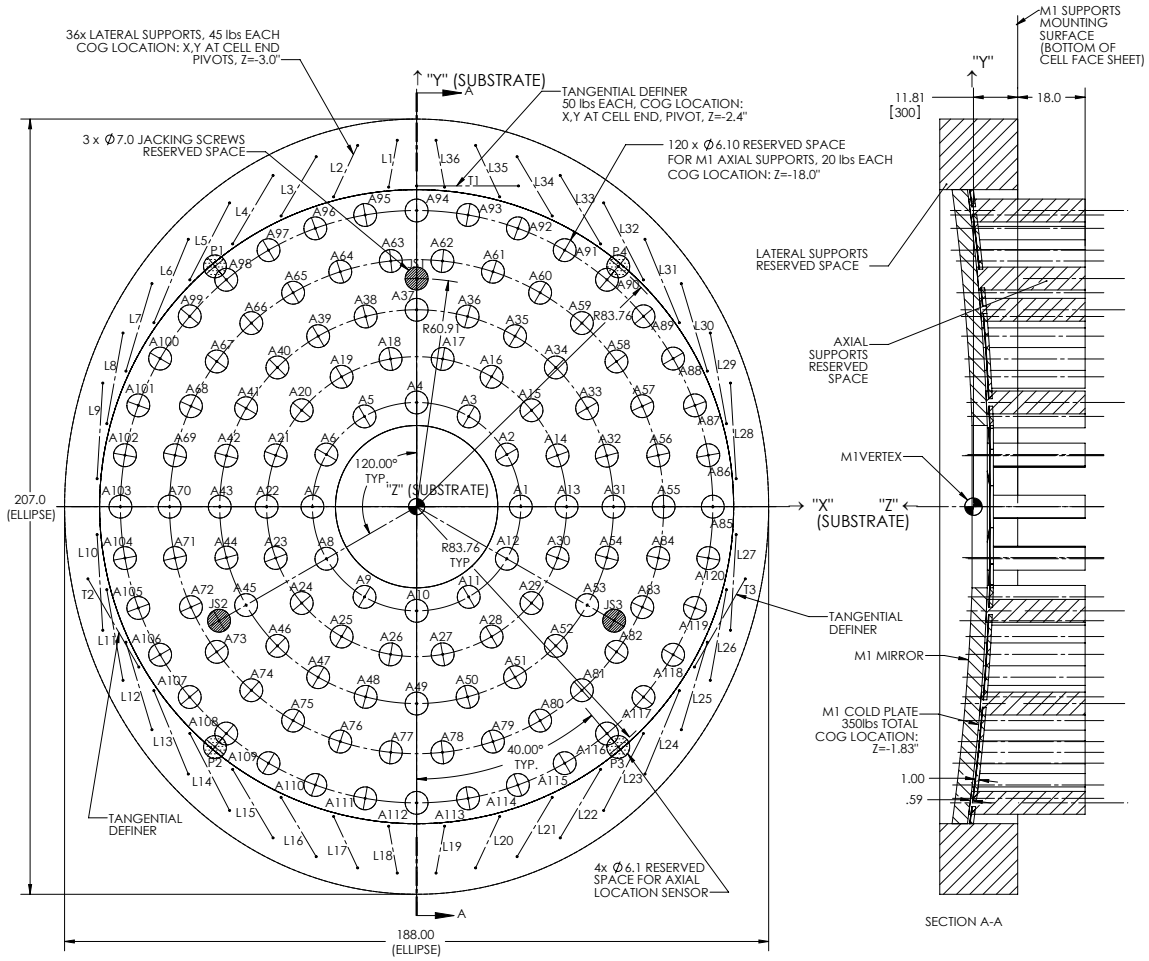

Figure 2. Layout of the M1 mechanical supports. The view is looking down on the primary mirror. The axial supports are arranged in 5 concentric rings; each actuator location is shown by a small open circle. The 36 lateral supports and three tangent definers are indicated by the numbered lines around the outer edge of the mirror. Finally, the three jack screw locations are shown by the gray filled circles.[9]

The secondary mirror is supported within an aluminum cell, using three axial definers, a central radial defining hub, and a tangent defining strap. Concentrated body forces on the glass are eliminated by floating the mirror

using a modest partial vacuum (approximately −0.25 psig). The entire cell is controlled in piston and tilt by three electromechanical actuators similar in design to those used for the primary mirror figure control. The cell is adjusted manually for centration using three tangential defining rods, an activity intended only to be performed immediately after the mirror is coated and installed.

2.2.1 M1 Figure

The primary mirror was delivered to the DCT site in the spring of 2010 after being figured by the University of Arizona Optical Sciences Center. The delivered radius of curvature is 15994.7 ± 0.129 mm, and the conic constant is -1.0828 ± 0.00009.[10] The mirror was polished in and out to aperture diameters of 1120 mm and 4280 mm respectively.[10] With the inner and outer stops installed, the clear aperture inner and outer diameters are 1200 and 4267mm.

The final optical axis of the polished surface was found to have been offset by 8.64mm with respect to the mechanical axis. In the end, we modified the M1 cell to account for the offset.[10]

The M1 was coated on site in January 2012.

Table 1. DCT Optical Constants

Constant [units]	Specified	As Built	Ref.
M1 Radius of Curvature [mm]	16000 ± 10	15994.42 ± 0.129	10
M1 Conic Constant	-1.0827 ± 0.0002	-1.0828 ± 0.00009	10
M1 Clear Inner Aperture [mm]	1200	1120	10
M1 Clear Outer Aperture [mm]	4200	4280	10
M2 Radius of Curvature [mm]	-6926.4 ± 0.5	-6925.79 ± 0.17	11
M2 Conic Constant	-4.5009 ± 0.0002	-4.500899 ± 0.0004	11
M2 Clear Inner Aperture [mm]	350		11
M2 Clear Outer Aperture [mm]	1340	1360	11
M1 to M2 vertex spacing [mm]	5619.05	5616.64	12
Bare Telescope Focal Length [mm]	25600	25586	
Effective Focal Length [mm] (with RC Corrector)	25960	25945	12

2.2.2 M2 Figure

The 1.4-meter secondary blank (M2) was made out of GE124 fused quartz and was provided in 2009 by Momentive Performance Materials, Inc. The blank back surface was 50% lightweighted by milling 85 pockets at Mindrum Precision in Los Angeles, CA (see Fig. 5, left). The front surface was roughly contoured by Optical Surface Technologies in Albuquerque. The figuring contract was awarded to L-3 Integrated Optical Systems – Brashear† in Pittsburgh, PA in 2010. The mirror was figured using magnetorheological finishing (MRF) technology which is exclusively available at L-3 Brashear. Prior to final polishing, the Invar center hub and three axial post inserts were precisely aligned and glued into the pockets in the back surface of the mirror. The figuring was completed in late 2011 along with attachment of four metrology Invar pucks to the outside diameter and sand blasting of a center mark in the middle of the mirror. The mirror optical surface was interferometrically tested using a Hindle shell and null lens in order to achieve full aperture coverage of the image.

With the final figure, 50% of the enclosed energy (EE) is within $0\farcs094$ diameter and 80% of EE is within $0\farcs27$ diameter. The surface quality was further verified by the independent structure function. Fig. 3 shows the required structure function of the mirror final figure as measured with loose mirror, with mirror mounted in the DCT cell, with astigmatism removed and including expected correctability. The cell was assembled with the

†This document includes L-3 Communications Corporation general capabilities information that does not contain controlled technical data as defined within the International Traffic in Arms Regulations (ITAR) Part 120.10 or Export Administration Regulations (EAR) Part 734.7-11.

mirror after the final polishing. Due to the zenith looking orientation of the mirror during the interferometric testing, the mirror was supported with positive air pressure counteracting the gravity forces, as opposed to the actual orientation of the mirror in the telescope when the cell is under partial vacuum.

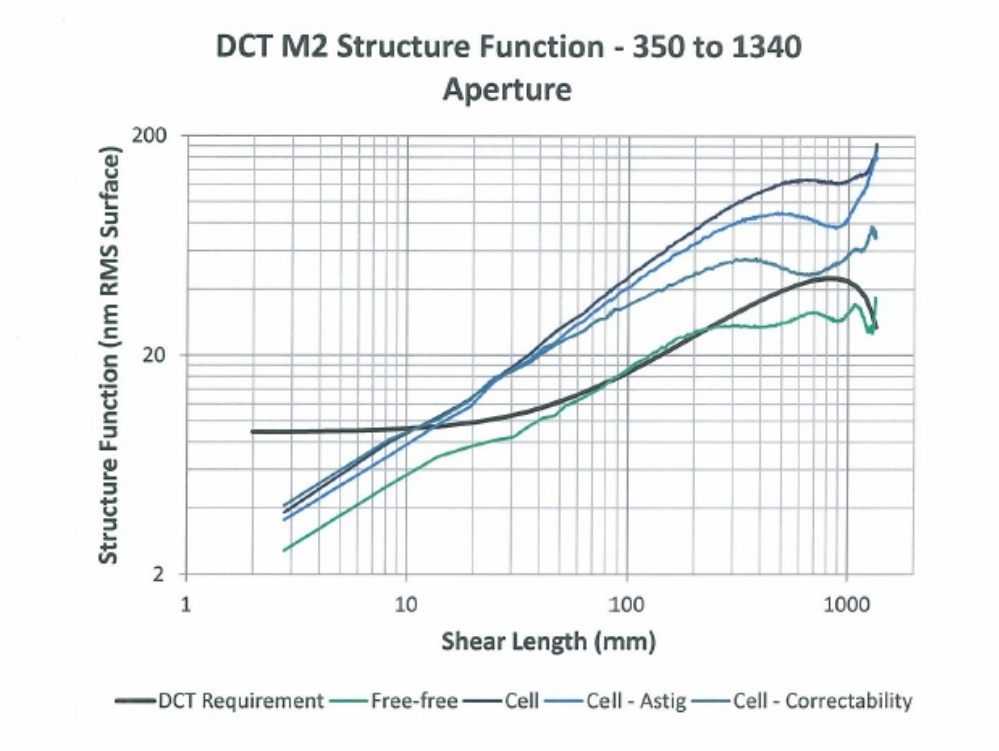

Figure 3. Optical surface structure function plotted over normalized distance (mirror surface error = $^1/_2$wavefront error). (Graphic courtesy of L-3 Communications.)

The optical surface error slightly exceeds the prescribed structure function in the 90-210 mm spatial length, mainly due to the test uncertainty in the 3rd-order spherical Zernike term. The cell installation error contribution roughly doubles the loose mirror surface error. The surface map for the aperture radius 1380mm was obtained by visible interferometry and is shown in Fig. 4 for the free mirror (left) and mirror mounted in its cell (right). The cell used positive air pressure to compensate for the gravitational forces on the mirror itself. The figured mirror has an as-made clear aperture up to 1360mm, radius of curvature 6925.79mm and < 2 nm RMS surface roughness.

2.2.3 M2 Cell Assembly and Alignment

The secondary mirror was delivered to the telescope site at Happy Jack, Arizona in late December 2011 and aluminized in the DCT coating chamber. The aluminized mirror was assembled into the cell. The mirror position in the cell was defined by three axial posts with titanium flexures and a central radial hub equipped with flexible membrane as seen in Fig. 5, left.

The proper function of the design depends on installing and aligning the membrane perfectly flat in the center hub assembly in order to minimize residual parasitic forces on the glass. The weight of the mirror itself is supported with partial vacuum in the cell, precisely controlled as a function of the telescope elevation angle. The three axial posts are equipped with force transducers, allowing precise control of the vacuum pressure. The target cumulative residual force must be maintained to less than 3.0 lb. The cell assembly is mounted at the front end of the top end frame structure using three manually adjustable tangential definers and three actuated axial rods. The axial rods provide precision positioning (piston and tilt) of the M2 cell assembly using three electromechanical Harmonic Drive actuators.

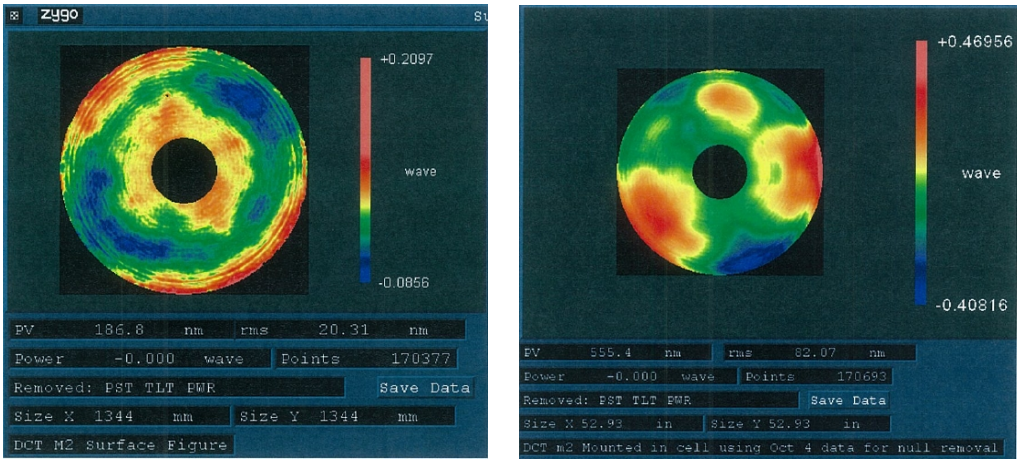

Figure 4. M2 as-figured surface maps. Loose mirror (left) and mounted in DCT cell with positive air pressure (right). The positive pressure was required to float the mirror in the cell for the up looking test; in real operations we will pull a vacuum. (Graphic courtesy of L-3 Communications.)

Figure 5. Left: Axial posts and radial hub assembled in the secondary mirror (M2). The holes for lightweighting the mirror are also clearly visible. Right: M2 backing plate assembly.

2.2.4 Installation and Alignment of M1 and M2 on DCT

The primary mirror was installed in its cell in July, 2011 after aluminizing. The first step in the installation was performed in the auxiliary building, placing the mirror on the axial jackscrews. The mirror cell was then transported to the telescope building for alignment of the mirror with the cell. The goals of aligning the mirror with the cell are to center the glass with the Cassegrain rotator centerline, level the mirror, and place the mirror vertex the correct distance from the Cassegrain rotator bearing (a surrogate for the focal plane). This was accomplished by means of a laser tracker which acquired measurements from sphere-mounted retro-reflectors (SMRs) located on the mirror and cell to determine the desired position. The mirror was lifted using the facility bridge crane, and roughly centered on the cell. Fine centering adjustments were made by connecting the tangent definers to the mirror with the mirror weight supported by the bridge crane.

The tangent definer adjusters (Fig. 2) were used to set the desired position of the glass in X and Y, and to achieve a neutral clocking position. When we were satisfied that the centration and clocking were correct, we raised the jackscrew restraints to take the mirror load and restrain the glass in the desired position. Small adjustments of the jackscrews allowed us to level the mirror.

Following mirror alignment with the cell, the axial supports were installed and adjusted, and the lateral supports, tangent definers, and axial position sensors were connected to the mirror pucks. When connections were completed, the jackscrews were lowered allowing the full mirror weight to be taken by the support system.

Daytime alignment of the secondary mirror on the telescope was performed in a similar manner to the primary mirror/cell alignment. The laser tracker was mounted on the mount elevation ring in a manner that afforded a view of SMRs on both mirrors. After acquiring the primary mirror SMRs, a coordinate system at the M1 vertex was established. Measurements of the secondary mirror then indicated adjustments in centration, X and Y tilt, and spacing to the primary mirror. The centration adjustments are made manually by adjusting tangent bars on the secondary mirror cell support structure. Tilt and spacing adjustments are made by moving the secondary mirror cell axial supports. The process iterated until satisfactory alignment was achieved. The resulting alignment was confirmed by use of an alignment telescope mounted in a fixture at the Cassegrain instrument cube location. This completed the daytime alignment process.

The plan for nighttime fine alignment is similar to that described by McLeod.[13] The first step in the process is removal of coma by tilting the secondary mirror about its vertex. This was accomplished initially by visual inspection of out-of-focus star images. For fine adjustment, the instrument cube wavefront sensing probe was used to measure the coma, and the M2 tilt was adjusted accordingly.

Because of the relative difficulty of making centration moves of the secondary, our plan is to adjust the centration only during laser tracker alignment. After that, any alignment adjustments (such as are made during normal operation at the command of the wavefront sensing system) will result only in tilt motions of the secondary mirror. Testing to date suggests the remaining alignment error with the centration fixed will be tolerable in terms of image quality. Measurements of field astigmatism, expected this summer, will indicate whether our plan to make only tilt adjustments is acceptable in terms of impact on the image quality.

2.3 Controls

The user's view of the functional organization of the ensemble of control systems needed to run the DCT is shown in Fig. 6. The DCT controls are largely written in LabVIEW and run on VxWorks real-time, FPGA and Windows 7 targets. The instrument control (including the guider and WFS) run under Linux and MacOSX. The UI layer is in java and is largely platform independent.

The telescope control system (TCS) was written by OSL; they wrapped the TPOINT/TCSpk pointing kernel inside LabVIEW for ease of integration with the rest of the DCT systems. The TCS communicates with the Mount Control System(MCS) by Ethernet. The MCS is comprised of a Mount Control Unit (MCU) which provides position demands to Power Drive Units (PDUs) for each axis over a dedicated Ethernet.

The PDUs contain the hardware and firmware required to close the position and velocity loops for each axis. Each PDU contains a dedicated microprocessor system that compares the demand with the position feedback from the on-axis transducers. The generated position error terms are frequency compensated and converted to rate commands. The rate command is compared with the motor rate feedback, and the error term is then used to direct motor controllers that deliver DC current to the motors.

For the AOS, LabVIEW applications[14–16] provide the system control needed to coordinate the mirror figure control and alignment tasks. Feedback is provided by linear incremental encoders for high-resolution position sensing, by linear variable differential transformers (LVDTs) for absolute position, and by high-resolution force transducers for loads.

3. COMMISSIONING

Commissioning of the telescope has been an extended process. As each new subsystem has come on-line, we have added it to the existing suite of system. Work testing out the mount and telescope control began as early as fall 2010. Even without optics, we were able to start characterizing the pointing and tracking performance of the mount.

Because the single most complex system on the telescope is the Active Optics System, we were anxious to begin testing on this as early as possible. To that end, we split the initial AOS testing into two phases, a prime focus phase where we were able to work with M1 alone, and then the RC focus phase, using the entire system (including M2).

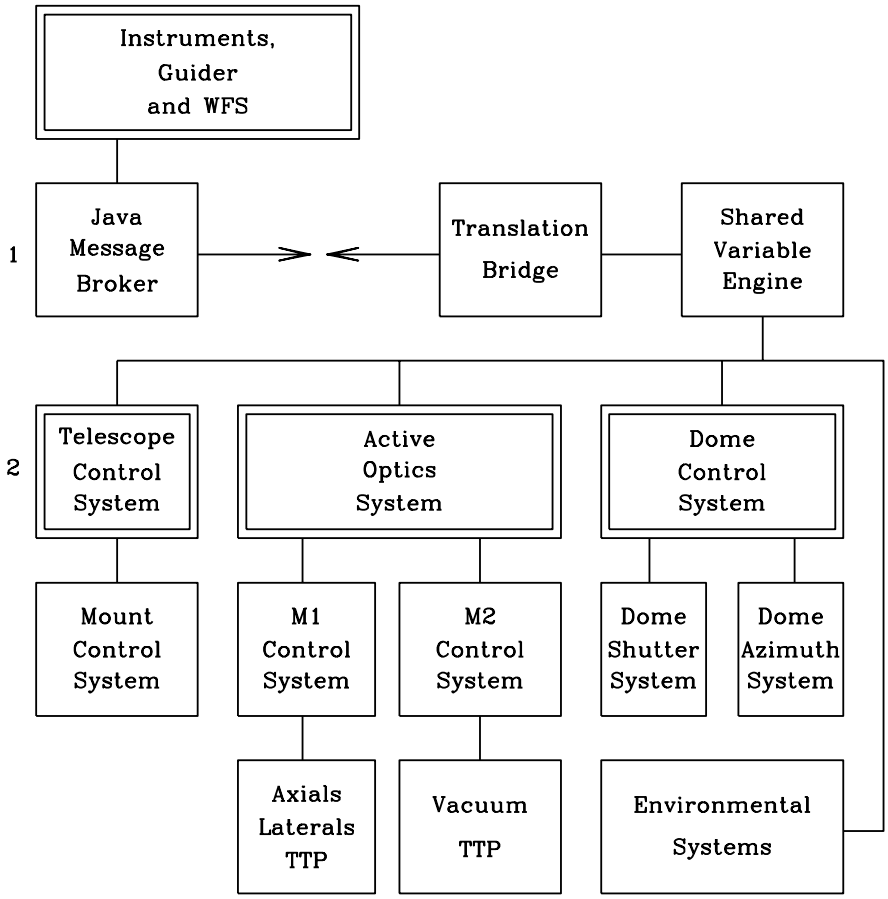

Figure 6. Overall functional organization of the DCT control systems. The bottom two lines are largely hardware and low level control. **TTP** refers to "Tip-Tilt-Piston", indicating the systems which control rigid body positioning of the M1 and M2. The line labeled **2** shows the top level major subsystem controllers. These are also the primary components that user will interact with, and may contain user interfaces. Line **1** has functions that are responsible for communications between all the DCT subsystems and between those and the instrument package (including the guider and wavefront sensor). The colliding arrows indicate the interface between systems that are considered telescope related, and those that are handled like instruments.

The DCT Active Optics System (AOS) maintains collimation and mirror figure to provide seeing-limited image quality. The AOS can operate open loop or closed loop. Open loop AOS operation maintains collimation and M1 mirror figure with operational parameters and calibration data (i.e., Wavefront Open Loop Model, abbreviated WOLM). Closed loop AOS operation maintains collimation and M1 mirror figure with combined WOLM and wavefront data. Collimation is maintained by converting Zernikes 4, 7, and 8 to piston, Y-Tilt, and X-Tilt, respectively (we follow the indexing convention of Noll[17]). M1 figure is maintained by converting Zernikes 5, 6, and 9 through 47 to 26 bending modes. In turn, the 26 bending modes are converted to a M1 axial support force suite. The AOS testing and performance are covered in greater detail in Ref. 18.

3.1 Prime Focus Testing

Because the primary mirror was ready for installation before the secondary mirror was complete, we constructed a temporary prime focus test camera. We used this to begin debugging the M1 support and control systems in September 2011, almost six months before M2 was ready. The lack of a secondary was actually an advantage; the optical system was one element simpler. The key elements that were tested were the various transformations in the chain of operations between the WFS and the AOS finally applying force to the M1. The WFS decomposes the wavefront into a finite set of Zernike polynomials. These are passed to the AOS, which transforms them into a different, finite set of flat plate Bending Modes.[19] Those modes are then used to construct the forces to be applied to each axial support behind the M1.[20]

The final system will use up to 47 Zernikes converted into 3 Zernikes and 26 Bending Modes. We have started with the low order subset that are analogous to focus, coma, astigmatism, trefoil and spherical. It is helpful that for most of these modes, there are close analogues in the Bending Mode solution space; the Zernike to Bending Mode transformations are not one to one, but close. By January 2012, when we began M2 installation, we had been able to demonstrate improvement in the image quality with a person doing the wavefront solution and feeding the result back into the AOS.[18]

3.2 RC Focus

After installing and aligning the M2, we have repeated the pointing model and AOS tests, this time with the WFS at the RC focus. The prime focus test work saved us a lot of time at this point, as we had most of the transformations correct.

4. INITIAL PERFORMANCE

4.1 Pointing And Tracking

Work on assessing the pointing and tracking performance of the mount began shortly after the mount was completed in late fall of 2010. A long focus 6inch refracting telescope on a solid optical bench was assembled and attached to the DCT elevation ring. With this, we were able to test both pointing and tracking accuracy and precision even though the optics were not complete. The first pointing model was made with this telescope.

Since then, we have constructed pointing models using the Prime Focus Test Assembly, which was mounted on the backside of the secondary mirror support cage. Most recently, we have constructed pointing models using the guider and wave front sensing cameras on the instrument cube at the RC focus. While we concentrate here on the most recent pointing results, it is interesting to note that the results done with all three setup have been pretty consistent with each other, even though there were significant changes in the telescope between them.

The expectation is that during normal operations, we will constantly add to the pointing model data set, and update the model on a regular basis. For the moment, we have concentrated on getting a good enough model to facilitate other commissioning activities. The current pointing map is based on 60 pointings taken over roughly three hours during one night in April 2012. This model has a bit of night to night drift of the zero points at the $\sim 10''$ level, but the other terms have proven quite stable over the past several months.

The mount is well enough behaved that we have so far limited our modeling to the geometric terms including the axis zero points and mis-alignments, and low order flexure terms depending solely on zenith distance. With this set, the model RMS is on the order of 1 to $2''$, and provides arcsecond level pointing from within a few degrees of the zenith down to roughly a zenith distance of 80° to 85°.

The mount shows a modest tilt of the azimuth pole from the vertical; when measured after installation with a laser tracker the total tilt was $6\farcs12$, which is similar to the values derived later from the pointing map of roughly $15''$ North-South and $1''$ East-West. The non-perpendicularities between the pointing axis, and the elevation axis and between the elevation and azimuth axes were measured with the laser tracker at $3\farcs6$ and $12\farcs6$ respectively. The corresponding terms derived from the pointing model are on the order of $70''$ and $20''$ respectively. While the discrepancies may seem large, it is important to note that the current pointing model does not account for things like non-concentricity of axes and such. More importantly, the derived pointing model terms have been quite stable and varied by very little over the course of the past year.

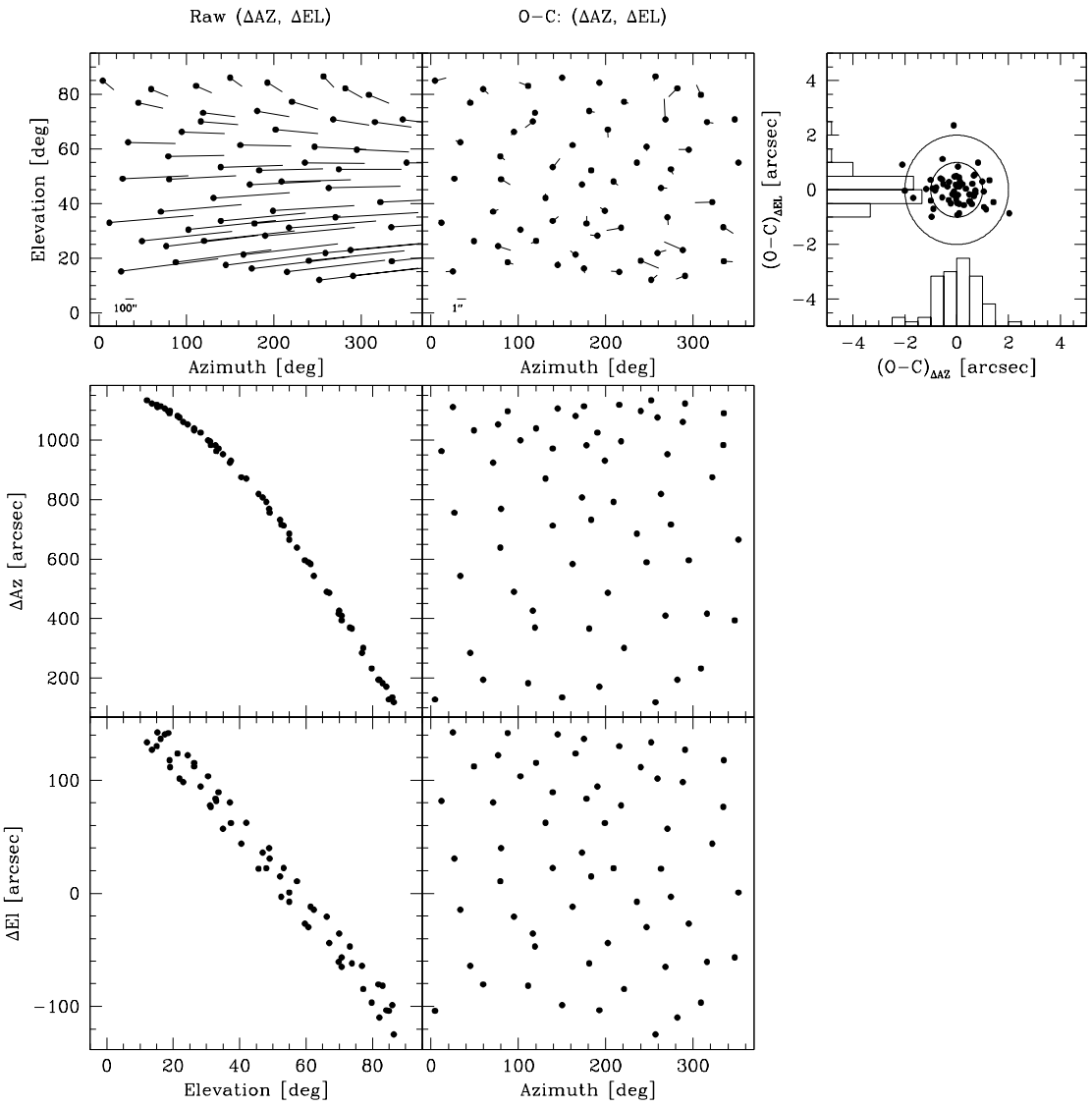

Figure 7. Pointing model data. *Upper left:* Raw difference between the requested azimuth and elevation and the actual azimuth and elevation. *Upper middle:* Differences between the requested azimuth and elevation, after correction for the pointing model, and the actual azimuth and elevation. *Upper right:* Plot of the residuals to the pointing model data. The concentric circles are 1 and 2″ in radius. The overall RMS for this model was less than 1″ in both azimuth and elevation. *Lower* 2×2 *plot:* Differences in the requested azimuth and elevations versus azimuth and elevation for the pointing model data.

The tube flexure as a function of zenith distance has turned out to be well modeled by a third order polynomial in zenith distance (including the linear and quadratic terms). This turns out give a slightly better fit than a combination of the classic sin and tan terms, but is very similar (which is not too surprising, since they are essentially the low order terms of the series expansion of the trigonometric functions; see Fig. 7, lower $2x2$ panels).

With this pointing model the mount can take unguided 5 minute exposures that show no evidence of drift,

though by 15 minutes, there is drift. We do expect that the pointing model will evolve as we acquire more data at a much wider range of night time temperatures.

4.2 AOS Test Results

The first (and deceptively simple) test that we tried was to track on a star, and while tracking turn off the AOS entirely and then re-initialize it. The pleasant result in multiple trial was that in all cases the stellar image came to within a fraction of an arcsecond of where it had been on the detector before we cycled the AOS.

4.2.1 AOS Prime Focus Test Assembly (PFTA) Testing

In the prime focus configuration, the AOS controls M1. AOS maintains M1 figure with bending modes and maintains collimation with rigid body motions of the M1 (tip, tilt and piston). With the PFTA and M1 installed, the AOS could bend M1 and the Wavefront Sensor (WFS) observed the changes in M1 figure. We manually put the WFS feedback into the AOS. Part of the testing included verifying AOS coefficient signs and amplitudes compared to the Zernike coefficients produced by the WFS. Testing identified the bending modes coefficients were opposite sign for the sine azimuthal functions. An important modification to the transformations from Zernikes to bending modes was to use bending modes 13, 16 and 17 instead of 2, 5 and 6. The key difference is that Bending Mode 13 is a much better match to Spherical than Bending Mode 2, which is a cone mode, and much more like focus. (The need to exclude one or the other trio is a result of delicate cancellation properties of some of the modes, making them almost degenerate in the presence of noise.)

As part of PFTA testing, we started collecting data for the WOLM. We performed elevation scans to collect data for the elevation dependent terms. The WOLM tool (linear regression analysis) converted the elevation and wavefront data into WOLM coefficients (i.e., slope and offset). The Cassegrain Instrument Assembly was installed before WOLM coefficient testing occurred.

4.2.2 Initial AOS with Cassegrain Instrument Assembly Testing

In the RC configuration, the AOS controls both M1 and M2. The AOS maintains M1 figure with bending modes and maintains collimation via rigid body modes (i.e., Zernikes 4, 7, and 8). We checked the AOS for correct signs and amplitudes used to convert Zernikes 4, 7, and 8 to piston, Y-Tilt, and X-Tilt, respectively. The first on-sky images showed very good results. The image quality ranged from $0\farcs9$ to $1\farcs1$ FWHM without any wavefront correction other than focus. With wavefront correction from Z4 (focus) to Z11 (spherical aberration), the image quality ranged from $0\farcs8$ to $1\farcs0$ FWHM.

In the process of implementing the correction loop by hand, we have found that the optical aberrations are reasonably stable over periods of ten to even twenty minutes. This was demonstrated empirically by our ability to do a WFS decomposition, send a correction, bend the mirror, and repeat the whole cycle multiple times and see progressively improved image quality. The stability of the system is already making the system easier to work with than we had feared, as we do not need to try to speed up our original 30 to 60 second correction cycle.

WOLM development continues with the Cassegrain Instrument Cube Assembly. We collected elevation scan data over a month. The data provided good input into the WOLM tool for elevation dependent terms. The WOLM coefficients for mount temperature need further development including a larger temperature range. Even with the limited data collected to date, we see solid trends in zenith distance and mount temperature for several Zernikes, especially focus and y-coma (Z4 and Z7 - see Ref 18 for more details).

4.3 Delivered Image Quality

Perhaps the most critical question we can ask is what does the delivered image quality look like in a typical science image? As noted in the previous subsections, we are seeing uncorrected image quality of roughly $1''$, in a small field of view on the optical axis. If we make the effort to correct that, we have been able to improve the FWHM by almost $0\farcs2$, which comes out to between $0\farcs4$ and $0\farcs6$ worth of aberration removed in quadrature. Fig. 8 shows a sample uncorrected and correct stellar image, and the corresponding radial profiles.

In a similar vein, we can ask what the image quality is like as we move away from the optical axis of the telescope. While the suite of first light instruments are still being worked on, we did borrow the CCD camera

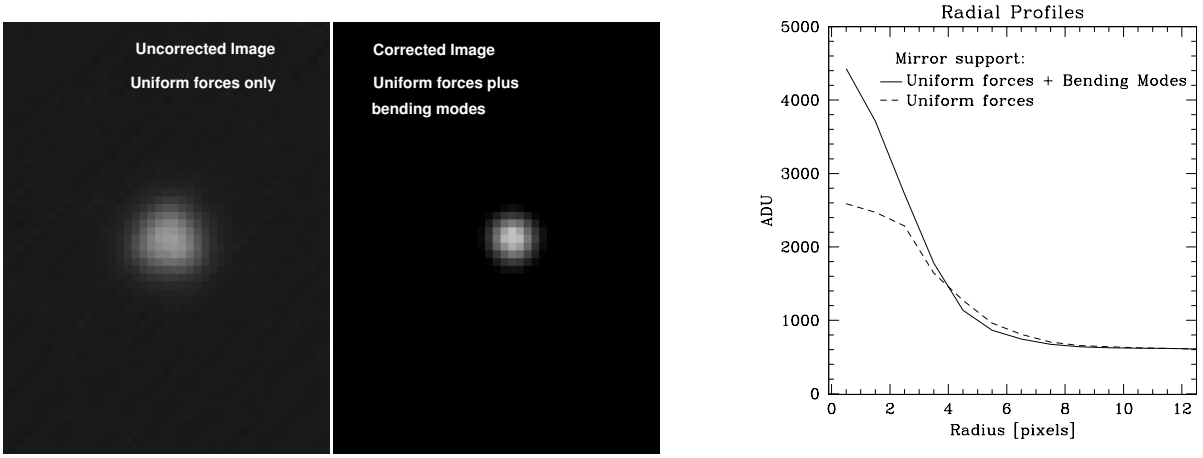

Figure 8. Stellar images taken with the prime focus test array with the primary mirror uniformly supported (left) and with corrective bending modes applied (middle). The radial profiles from the two stellar images show noticeable improvement when the mirror is bent to correct for aberrations (right).

used on the Lowell 1.1-meter Hall telescope. The CCD is a 4K × 4K e2v CCD231, with 15μm square pixels. This is the same architecture as the CCD that will be used in the workhorse optical imager, the LMI (see below), but 2/3 the linear dimension. Hence, the field of view is roughly $8' \times 8'$, instead of the $12\farcm5 \times 12\farcm5$ that we will use. This is big enough to permit us to make an initial assessment of the image quality off axis.

Fig. 9 shows an R band image of NGC 5466 taken at the RC focus in April of 2012. The field of view is smaller, BUT, the RC corrector had not yet been installed (that was done in mid-June). The image FWHM was slightly less than $0\farcs8$ (radial profiles for stars near the corners are shown in Fig. 9).

5. FIRST LIGHT INSTRUMENTS

Over the next 6 to 12 months, DCT we expect to install the first set of science instruments at the DCT. All will be mounted on the Cassegrain Instrument Assembly, which is capable of carrying up to 5 instruments. Instruments can be selected using pick-off mirrors in the cube, thus making it easy to switch between various instruments in a matter of minutes.

5.1 Cassegrain Instrument Assembly and GWAVES

While not strictly speaking an instrument, the Cassegrain Instrument Assembly is at least as complex as most instruments, and critical to the efficient operation of the DCT (see Ref 21 for more detail). The cube contains two identical CCD cameras on movable stages. Each probe can be used as either a guider or wavefront sensor. The CCD on each is an e2v CCD67, a 256 × 256 pixel, frame transfer device. The field of view is roughly $92'' \times 92''$, and each is equipped with 2 Shack-Hartmann lenslet arrays (fine and coarse) and a set of broad band filters.

The straight through path goes through a low power, two element corrector, which gives a $30'$ diameter corrected field. Out of that, the central $12\farcm5$ square will be imaged by the Large Monolithic Imager (see § 5.2). The region outside that will be used by the guider and wavefront sensor. The LMI shutter is a Bonn Shutter and is mounted on the bottom plate of the cube, and below that sits the LMI filter wheel. The filter wheel contains two 10 slot filter wheels.

The four side ports are fed by pick-off mirrors that can be inserted into the beam above the corrector. One port currently has a focuser, permitting use of both commercial cameras, and an eyepiece. The cube is already assembled and mounted on the telescope.

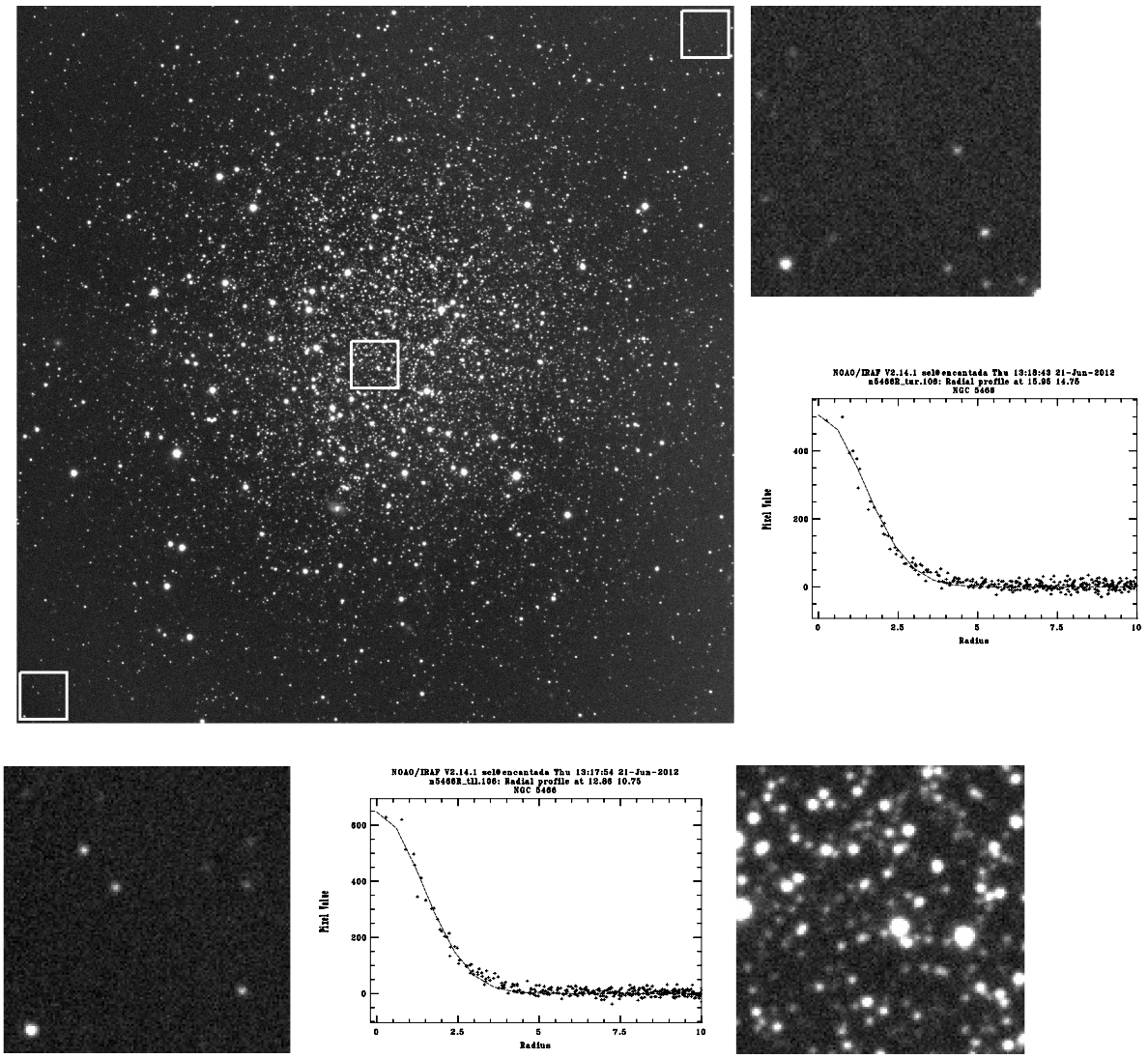

Figure 9. R band image of the globular cluster NGC 5466 taken with the DCT using Lowell Observatory's NASA42 camera. The field of view is roughly 8′ on a side. Enlarged subimages (delineated by the white squares) from the lower left, center and upper right of the original image are spaced around the main image. For the lower left and upper right images, there is also a radial profile for the brightest object in the subframe (in both cases, the star in the lower left).

5.2 LMI

The Large Monolithic Imager (or LMI) is being led by P. Massey and is expected to be the primary optical imager for the DCT. The detector will be an e2v CCD231 6.1K × 6.1K CCD, with 15μm square pixels. The on-sky field of view will be 12.′5 × 12.′5. By having a single large device, the DCT will not need to dither to fill in the gaps as would be necessary with a mosaic camera. This is especially important for projects that involve very low surface brightness extended regions (like the outer reaches of dwarf galaxies, and the comae of comets).

The instrument is coming along well. The dewar has been assembled and leak checked. The electronics have been procured and most of the internal parts for mounting the CCD have been fabricated. The camera uses a Stirling cycle cooler. The vibration damping mounting has already been designed, fabricated and tested. The CCD for the camera is in final testing now (June 2012) at e2v and we expect delivery shortly. The camera could

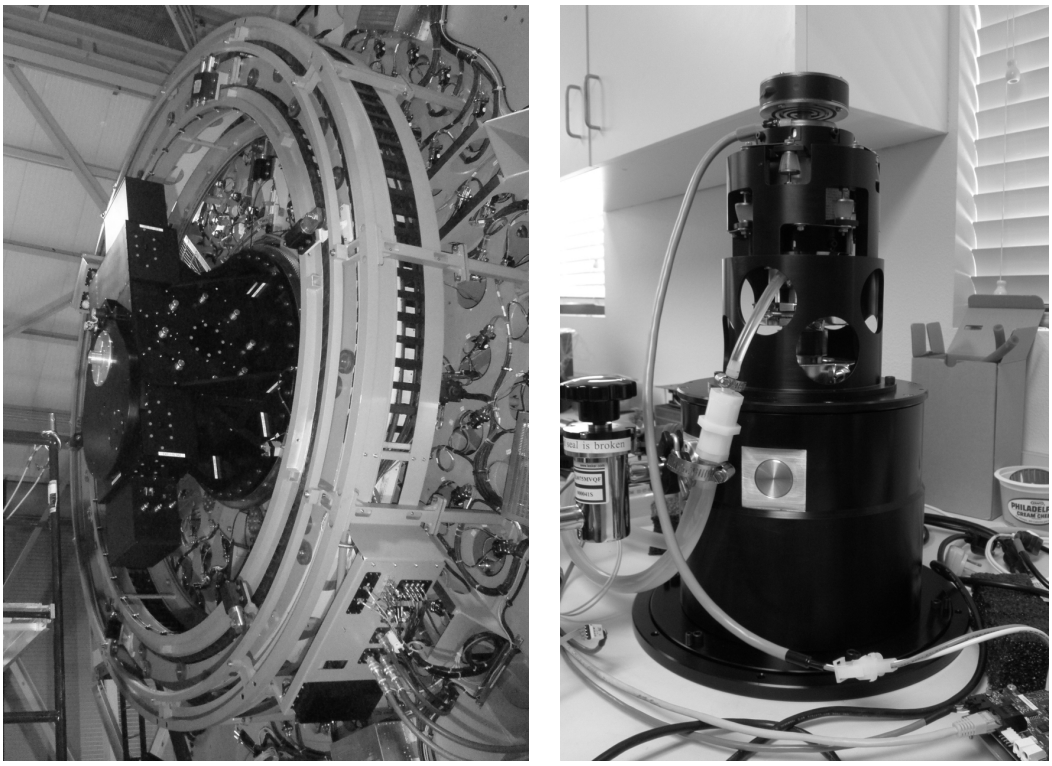

Figure 10. *Left:* The Cassegrain Instrument Assembly mounted on the back of the DCT. The round silver plate in the middle of the cube face is a fixture to hold the alignment telescope. It is attached to the backside of the LMI filter wheel. *Right:* The LMI dewar in the Lowell instrument lab during assembly and testing.

be ready to test on sky by mid-summer 2012.

5.3 NIHTS

The other new instrument being built as part of the first light suite of instruments is the Near IR High Throughput Spectrograph (NIHTS). NIHTS will cover roughly 0.9 to 2.4μm in one exposure at a resolution of 200. This effort is being led by H. Roe. Detectors, electronics and optics have all been procured. The mechanical design is well advanced, and the dewar is expected to be put out to bid by early summer 2012.

NIHTS will be mounted on one of the folded ports of the RC instrument cube. Instead of using a fold mirror, it will be fed by a dichroic, thus allowing simultaneous optical imaging and near IR spectroscopy of targets.

5.4 DeVeny Spectrograph

To provide an optical spectroscopy capability, we are planning to move the existing DeVeny spectrograph (the old KPNO white spectrograph) from the Lowell 1.8-meter to the DCT. To do so will require minor modifications to the re-imaging optics, which are in the design stage now.

6. UPCOMING EVENTS

DCT has already seen first light (e.g. Fig. 9), and we are now pushing on to bring the system to science operations. Given the current state of the telescope and its control systems, and the progress being made on the first light instruments, we are anticipating first science operations during the early part of 2013.

ACKNOWLEDGMENTS

These results made use of the Discovery Channel Telescope at Lowell Observatory. Lowell is a private, non-profit institution dedicated to astrophysical research and public appreciation of astronomy and operates the DCT in partnership with Boston University, the University of Maryland and the University of Toledo.

The Discovery Channel Telescope would not be the reality it is without the vision and assistance of many people and organizations. In particular, we would like to thank W. L. Putnam, J. Hendricks and Discovery Communications, also R. Millis and J. Giovale. We also gratefully acknowledge the constant support of the Lowell Observatory Advisory Board. The NSF has funded the construction of the LMI (under grant AST-1005313). NIHTS is funded by a grant from NASA's Planetary Astronomy and Planetary Major Equipment programs. The DCT is sited on land in the Coconino National Forest of the US Forest Service, and we are delighted to acknowledge their willingness to work with us.

REFERENCES

[1] Wallace, P. T., A rigorous algorithm for telescope pointing, Proc. SPIE 4848, 125-136 (2002)

[2] Bida, T. A., Dunham, E. W., Bright, L. P, Corson, C., Site testing for the Discovery Channel Telescope, Proc. SPIE 5489, 196-206 (2004)

[3] Marshall, H. K., Teran, J. U., Bond, K., Design and construction of the Discovery Channel Telescope enclosure, Proc. SPIE 7733, 169 (2010)

[4] Marshall, H. K., Ash, G. S., Parsley, W. F., The Discovery Channel Telescope optical coating system, Proc. SPIE 7733, 7733E (2010)

[5] Finley, D. T., Squires, C., McCreight, B. A., Smith, B. W., Chylek, T., Venetiou, A., Design of the Discovery Channel Telescope mount, Proc. SPIE 7012, 70124I (2008)

[6] Smith, B., Chylek, T., Degroff, B., Finley, D., Hall, J., Lotz, P. J., McCreight, B., Venetiou, A., The Discovery Channel Telescope: early integration, Proc. SPIE 7733, 77330A (2010)

[7] Smith, B., Chylek, T., Cuerden, B., Degroff, B., Lotz, P. J., Venetiou, A., The active optics system for the Discovery Channel Telescope, Proc. SPIE 7739, 77391T (2010)

[8] Schwesinger, G., Lateral support of very large telescope mirrors by edge forces only, JMOp, 38, 1507 (1991)

[9] Chylek, T., M1 Supports Mechanical Interface (drawing), DCT-0440D-009-D (2008)

[10] University of Arizona College of Optical Sciences, Discovery Channel Telescope Primary Mirror M1 Final Report, DCT-0305R-026-1 (2010)

[11] Chylek, T., Secondary Mirror Figuring Specification, DCT-0315S-001-3 (2012)

[12] Burge, J., Re-optimization of DCT Cassegrain design for as-built primary mirror, DCT-0350A-0140A (2009)

[13] McLeod, B. A., Collimation of Fast Wide-Field Telescopes, PASP, 108, 217 (2010)

[14] Lotz, P. J., Greenspan, D., Godwin, R., Taylor, P., Discovery Channel Telescope software development overview, Proc. SPIE 7740, 77401M (2010)

[15] Lotz, P. J., Discovery Channel Telescope software key technologies, Proc. SPIE 7740, 77400O (2010)

[16] Lotz, P., Lacasse, M, Godwin, C., Discovery Channel Telescope software component template and state design: principles and implementation, Proc. SPIE 8451-07 (2012)

[17] Noll, R., Zernike polynomials and atmospheric turbulence, JOSA, 66, 207 (1976)

[18] Venetiou, A. J., Bida, T. A., Discovery Channel Telescope Active Optics System Early Integration and Test, Proc. SPIE 8444-49 (2012)

[19] Smith, B., M1 Bending Mode Analysis, DCT-0360A-007-A (2008)

[20] Smith, B., Cuerden, B., Bending Modes for Active Optics, Proc. SPIE 8149, 81490D (2011)

[21] Bida, T. A., Dunham, E. W., Nye, R. A., Design, development, and testing of the DCT Cassegrain instrument support assembly, Proc. SPIE 8444-192 (2012)